Entrance channel effect for complete fusion of O + C isotopes

B. Heusch, C. Beck, J. P. Coffin, P. Engelstein, R. M. Freeman, G. Guillaume, F. Haas, and P. Wagner

Centre de Recherches Nucléaires et Université Louis Pasteur, 67037 Strasbourg Cedex, France

(Received 1 December 1981)

The cross section for total fusion of the reaction $^{18}O + ^{12}C$ was studied over a large range of energies from near the Coulomb barrier B_C to $\sim 6B_C$. Good agreement was found between the critical angular momenta deduced from the experimental results and the predictions of different models. The reaction $^{17}O + ^{13}C$, leading to the same compound nucleus ^{30}Si, was studied in the second fusion region (above $\sim 2B_C$). By comparing the relative cross sections for fusion-evaporation to each isotope it is shown that for different entrance channels, even at the highest energies studied, the reactions appear to pass by the formation of a compound nucleus. The critical angular momenta were found to be systematically different from $^{18}O + ^{12}C$. This difference, which may be due partially to the entrance channel spin, is interpreted as arising from the effect of direct reactions diverting flux from the compound nuclear processes.

NUCLEAR REACTIONS ^{16}O, ^{17}O, and ^{18}O beams on ^{14}C, ^{13}C, and ^{12}C targets, respectively; natural and enriched targets; $E_{lab}=32$ to 140 MeV; time of flight with Z identification technique; fusion evaporation and direct cross section measurements from $Z=5$ to 14 and $A=10$ to 29; statistical model calculations; entrance channel effects discussed; macroscopic model results for total fusion cross sections.

INTRODUCTION

The phenomenon of the saturation of the cross section for complete fusion (σ_{fus}) at higher incident energies has occupied both experimentalists and theoreticians for about ten years. For the light systems which have been studied,[1-4] two distinct regions are clearly apparent when σ_{fus} is plotted as a function of $1/E_{c.m.}$.

In the low energy region ($B_C \lesssim E_{c.m.} \lesssim 2B_C$) the total reaction cross section σ_R is mainly σ_{fus}, and σ_{fus} decreases linearly with $1/E_{c.m.}$. This behavior is explained by the combined effects of the Coulomb and centrifugal barriers. At $E_{c.m.} \simeq 2B_C$ a change in slope occurs where σ_{fus} saturates, and this has been interpreted[5-7] by requiring the incident ions to reach a critical distance R_c in order that fusion can occur. In this second region σ_{fus} has been observed experimentally to vary linearly with $1/E_{c.m.}$ but the slope should now depend essentially on the nuclear potential at this critical distance. A quite different approach, where σ_{fus} is limited by the properties of the compound nucleus rather than the dynamics of the entrance channel, has been recently proposed by Lee *et al.*[8] They introduced a "statistical yrast line" along which the density of high spin states is high enough that the decay of the compound nucleus remains sufficiently competitive. At higher energies still a third region should appear where σ_{fus} drops rapidly due to the lack of formation of the compound nucleus. Certain experimental indications[2] for this region have been well reproduced by the rotating liquid drop model[9] (RLDM), as has been the case generally for heavier systems.

In this work we have been concerned with determining whether it is the entrance channel or a consequence of the properties of the compound nucleus which has the greatest influence on limiting the mechanism of fusion at the higher energies.

In this framework we have undertaken the study of the decay of the compound nucleus ^{30}Si over a wide range of excitation energies formed by the entrance channels $^{18}O + ^{12}C$, $^{17}O + ^{13}C$, and $^{16}O + ^{14}C$, and have looked for any entrance channel effects in the second region by comparing σ_{fus} for the first two of these systems. This study extends to higher energies than those undertaken at Argonne[10] ($^{18}O + ^{12}C$) and at Saclay[4] ($^{17}O + ^{13}C$).

These experiments have involved the measurement of the cross section for the formation of heavy

fragments using the technique of time-of-flight associated with Z identification. Such an analysis, where all isotopes have been separately identified, has never previously been done for these systems. It proved indispensable for the interpretation of systems like O + C where evaporation channels, like $3\alpha\chi n$, feeding the oxygen isotopes used as projectile, open at high energies and become an important contribution to σ_{fus}.

EXPERIMENTAL PROCEDURE

The MP tandem at Strasbourg has recently been upgraded to a maximum terminal voltage of 16 MV. This enabled us to work with ^{18}O and ^{17}O beams of $E_{lab}=140$ MeV corresponding to a machine voltage of 15.6 MV for completely stripped oxygen ions. Under these conditions beam intensities in the vicinity of 10 to 15 particle nA were obtained.

The experimental details concerning the time-of-flight spectrometer with ionization chamber for Z identification and the targets we have used, have already been described elsewhere.[11] For the ^{13}C targets we used a 99% enriched ^{13}C isotope to obtain self-supporting targets of 80 $\mu g/cm^2$ thick. From the elastic scattering data the effective ^{12}C contamination was found to be 2%. Figure 1 shows typical spectra for Z and mass obtained for the ^{17}O (140 MeV) + ^{13}C reaction. It is clearly seen that the resolutions in time, energy, and energy loss in the ionization chamber (200 ps, 0, 3% and 5%, respectively) are sufficient to isolate all the isotopes formed.

The angular distributions were in general measured between $\theta=3°$ and 8° in steps of 1° and at $\theta=10°$, 12°, 15°, and 20°. The absolute normalizations for the cross sections were determined from the elastic scattering. The optical model potential for the $^{18}O + ^{12}C$ system was chosen with great care and the experimental results cover a large range of incident energies: 32 MeV $\leq E(^{18}O) \leq$ 140 MeV. For light systems Gobbi[12] has proposed shallow imaginary potentials (weakly absorbing) with a linear energy dependence. The code GENOA[13] was used for the calculations with the parameters given in Table I. These values are the parameters given by Webb[14] adjusted to fit the present data. As shown in Fig. 2 the fit is quite satisfactory both for $^{18}O + ^{12}C$ as well as for $^{17}O + ^{13}C$ for which we have used the same potential. In the region where our results for $^{18}O + ^{12}C$ overlap with those of Sperr *et al.*[10] ($E_{lab} < 70$ MeV), the absolute values for σ_{fus} are in excellent agreement.

EXPERIMENTAL RESULTS

Our experimental results will be presented according to two aspects: the statistical decay of the compound nucleus ^{30}Si formed by one of the three entrance channels $^{18}O + ^{12}C$, $^{17}O + ^{13}C$, and $^{16}O + ^{14}C$; and the energy dependence of the absolute values of the cross section for the fusion process.

These cross sections were obtained by integrating the angular distributions of the evaporation residues over the whole angular range (Fig. 3). The greatest uncertainty arises from the optical model fit on which our absolute normalizations depend and this is estimated as ~6%. In comparison, the systematic errors inherent in the extrapolations necessary over the angular ranges are small (1 to 2%) and the statistical errors negligible (< 1%).

The results for the absolute cross sections are summarized in Table I including the subtotal for fusion products $Z \geq 9$. It should be noted that the cross sections for $Z \leq 8$, essentially the $3\alpha\chi n$ channels, become very important for excitation energies above 60 MeV in ^{30}Si.

The energy spectra for F, Ne, Na, and Mg which

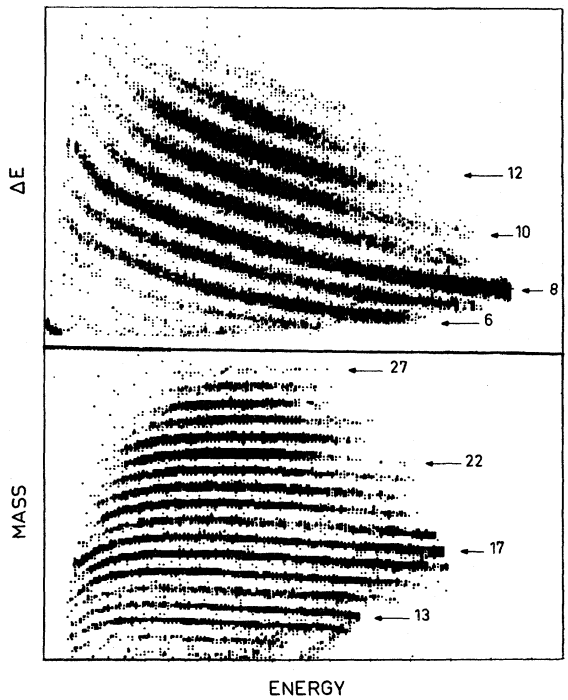

FIG. 1. Two dimensional energy loss (ΔE) and mass versus energy spectra measured with the ionization chamber and the time of flight system, respectively, for the $^{17}O + ^{13}C$ reaction at $E_{lab}=140$ MeV and $\theta_{lab}=8°$. Some typical Z and mass numbers are indicated.

TABLE I. Summary of the experimental results.

E_{lab} (MeV)	$E^*(^{30}Si)$ (MeV)	$l_g^{calc}(\hbar)$[b]	$\sigma_{reaction}^{calc}$[a,b]	$\sigma_{F.E.}^{exp}$ $(Z \geq 9)$[a]	$\sigma_{F.E}^{exp}$ $(Z \leq 8)$[a]	$\sigma_{total\ fusion}^{exp}$[a]	$l_{cr}^{exp}(\hbar)$[c]
				$^{17}O + {}^{13}C$			
54.09	50.19	17.9	1296	1010±60		1010±60	15.3±0.5
63.46	54.25	20.1	1383	990±60		990±60	16.5±0.5
76.00	59.68	22.7	1466	930±55	40±10	970±60	17.9±0.6
85.39	63.75	24.4	1514	810±45	125±30	935±65	18.7±0.7
103.84	71.75	27.6	1584	700±40	200±50	900±75	20.3±0.9
120.00	78.75	30.1	1630	640±40	210±50	850±80	21.3±1.0
130.00	83.08	31.6	1654	560±40	220±50	780±80	21.2±1.1
140.00	87.42	33.1	1675	510±30	240±60	750±75	21.6±1.1
				$^{18}O + {}^{12}C$			
32.00	36.45	10.0	788	700±70		700±70	8.9±0.5
35.00	37.65	11.1	887	876±50		876±50	10.6±0.4
38.00	38.85	12.2	968	977±45		977±45	11.8±0.3
41.50	40.25	13.3	1047	993±50		993±50	12.4±0.4
45.50	41.85	14.4	1121	1038±45		1038±45	13.4±0.3
49.50	43.45	15.5	1182	1178±40		1178±40	15.0±0.3
53.50	45.05	16.5	1234	1172±45		1172±45	15.6±0.3
70.00	51.65	20.0	1384	1093±55		1093±55	17.4±0.5
85.00	57.65	22.8	1471	1065±60	25± 5	1090±65	19.2±0.6
100.00	63.65	25.3	1534	885±50	125±20	1010±70	20.0±0.5
110.00	67.65	26.8	1567	770±50	170±30	940±70	20.3±0.7
120.00	71.65	28.3	1596	810±50	190±30	1000±60	21.9±0.7
130.00	75.65	29.7	1621	690±40	230±40	920±50	21.9±0.6
140.00	79.65	31.1	1643	645±40	245±40	890±50	22.4±0.6

[a]All cross sections are given in mb.

[b]Optical model calculation with the following parameters: $r_{Coul}=1.35$ fm; $V_R=17.0$ MeV; $r_R=1.35$ fm; $a_R=0.49$ fm; $W_I=1.25+0.67E_{c.m.}$ (MeV); $r_I=1.35$ fm; $a_I=0.35$ fm.

[c]l_{cr} values using the sharp cutoff approximation: $\sigma_{total\ fusion}^{exp}=\pi\lambda\!\!\!^{-2}(l_{cr}+1)^2$ with $\lambda\!\!\!^{-1}=0.218\,728\sqrt{\mu E_{c.m.}}$; μ: reduced mass.

are shown in Fig. 4 all have a broad contribution characteristic of evaporation residues. The higher energy contribution which appears for F and Ne corresponds to a more direct process (transfer of nucleons and an α particle, respectively) with a velocity close to that of the projectile. The two mechanisms are less readily separated when the fragments have the same Z as the projectile, but we have been aided by the M identification by time-of-flight. This is illustrated in the case of ^{17}O from the $^{18}O + {}^{12}C$ reaction at $E_{lab}=140$ MeV and $\theta_{lab}=5°$ in Fig. 5. An additional error of 10% has been included in the corresponding cross sections to take into account the uncertainties involved in making the cut. We have not, of course, been able to estimate directly the contribution for the isotope which is the same as the projectile. This is a crucial problem and the way it has been dealt with constitutes an original feature of this work. However, we have the results for both reactions $^{18}O + {}^{12}C$ and $^{17}O + {}^{13}C$, where the cross sections to common fusion channels are similar. Results for the $3\alpha\chi n$ channels for both reactions are shown in Fig. 6 and the good agreement for ^{16}O can be seen. In this way, an estimate could be made for the cross section which could not be measured experimentally and the total cross sections for the $3\alpha\chi n$ channels are listed in Table I. The cross sections of these channels are considerable and for $E^*(^{30}Si) \geq 75$ MeV represent $\simeq 30\%$ of σ_{fus}. In addition we have been able to estimate, in the case of the ^{17}O (130, 140 MeV) + ^{13}C reaction, contributions of 10±10 and 30±20 mb, respectively (included in Table I), for the $4\alpha\chi n$ evaporation channels leading to car-

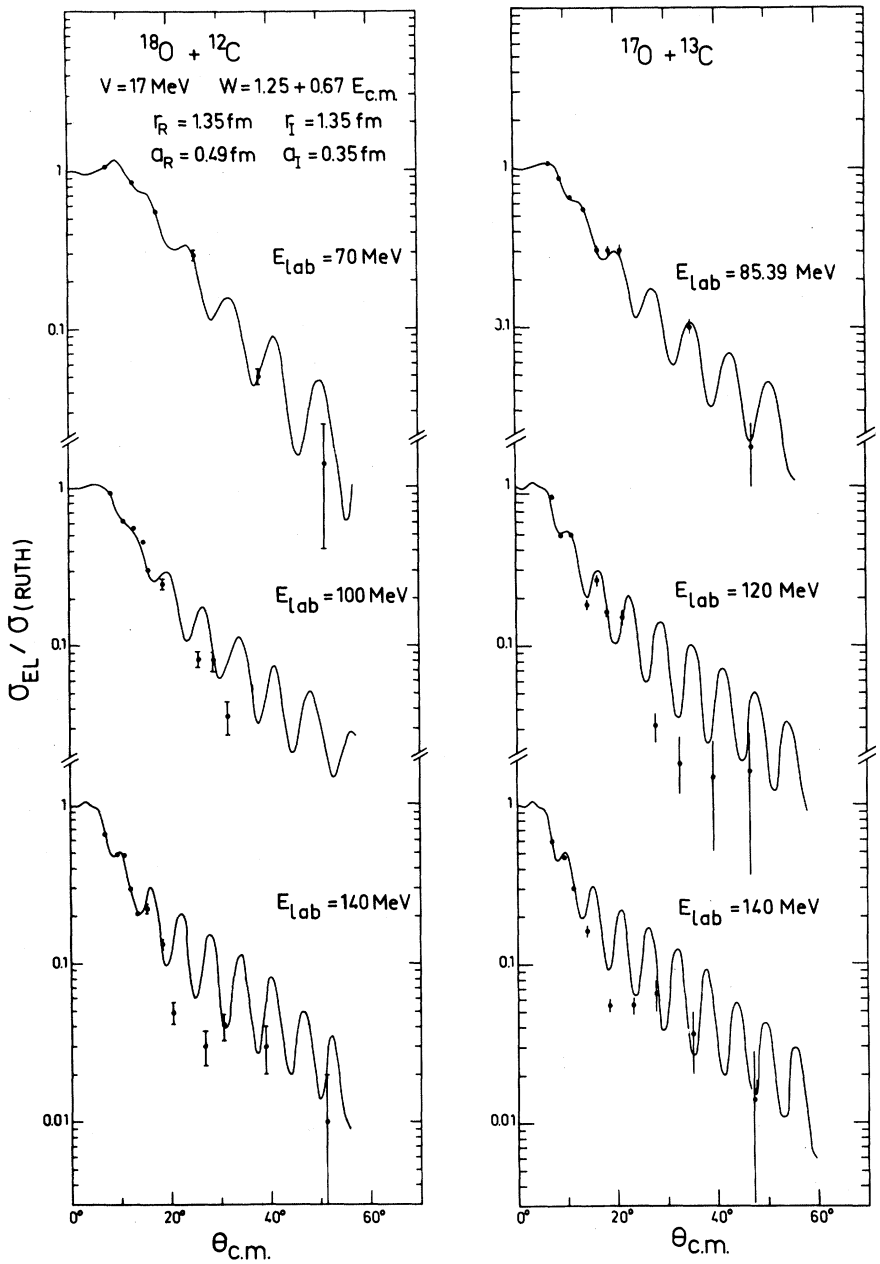

FIG. 2. Elastic scattering data measured at the indicated bombarding energies for the $^{18}O + ^{12}C$ and $^{17}O + ^{13}C$ reactions. The full lines are optical model fits using the code GENOA with the same parameter set for both systems.

bon isotopes.

In order to study the statistical decay of the compound nucleus ^{30}Si we have shown in Fig. 7 the relative values of the cross sections for the different elements formed as a function of incident energy. Considering the results which have been obtained for $^{18}O + ^{12}C$ (including our earlier measurement[15]) two regions appear:

(a) As we have recently shown,[16] below $E_{c.m.} \simeq 40$ MeV all channels change rapidly, as opposed to C + C systems for which the channels which decay by the evaporation of nucleons only evolve more slowly than αXn and $2\alpha Xn$.[11] In addition, for $E_{c.m} < 30$ MeV, the αXn channels feeding Mg isotopes dominate, although for the $^{16}O + ^{12}C$ reaction it is the $^{20}Ne + 2\alpha$ channel which dominates and by itself it is able to remove the high angular momentum over the same energy range.

(b) Above $E_{c.m.} \simeq 40$ MeV all channels change

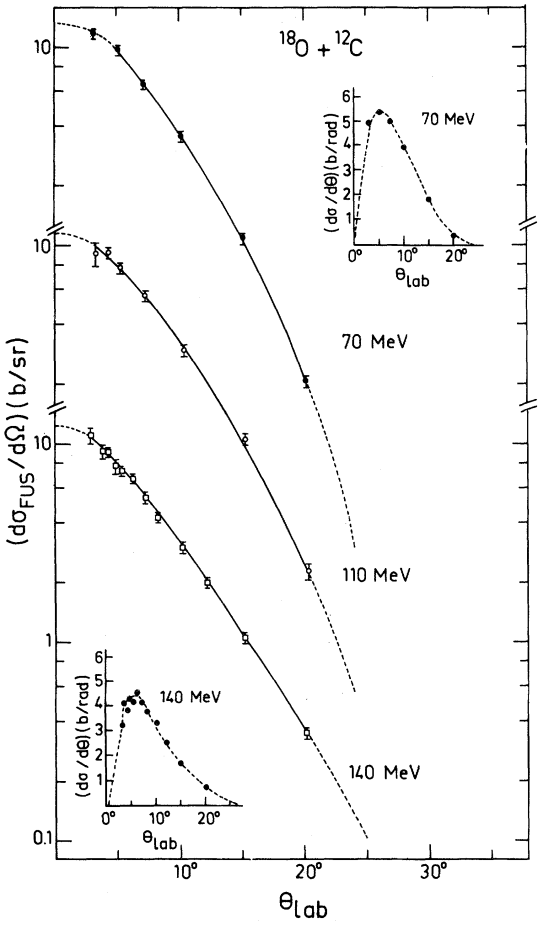

FIG. 3. Total fusion angular distributions measured for the $^{18}O + ^{12}C$ reaction at three bombarding energies.

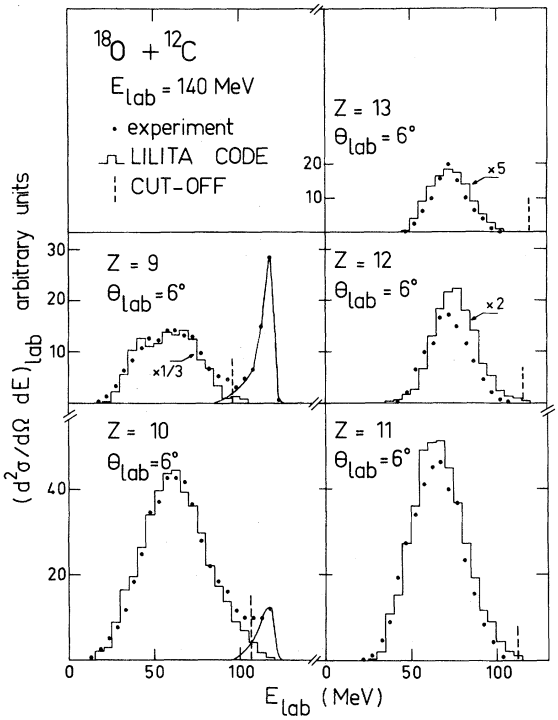

FIG. 4. Kinetic energy spectra for element fusion evaporation products for the $^{18}O + ^{12}C$ reaction at $E_{lab} = 140$ MeV and $\theta_{lab} = 6°$. The histograms are the results of the LILITA Hauser-Feshbach statistical model calculations. The considered energy cutoffs between direct and compound components are indicated.

less rapidly and finally decrease slowly with energy. The channels $2\alpha p\chi n$ and $3\alpha\chi n$ towards F and O are wide open and the evaporation of many particles (high multiplicity) allows a better removal of the higher angular momenta.

The fact that the feeding of the different channels remains fairly stable in this region is well illustrated by the Ne isotopes which are individually shown in Fig. 8. At high energy the marked increase in the number of open channels, as for example $^{23}Ne + \alpha 3$nucleons which opens at $E \simeq 35$ MeV, results in the replacement in the decay chain leading to ^{22}Ne, of an α particle by the successive evaporation of four nucleons which can carry away more angular momentum. Hence the second rise in the cross section $^{22}Ne + 2$"α".

In comparing the results for $^{17}O + ^{13}C$ and $^{18}O + ^{12}C$ no measurable effect of the entrance channel appears either at low energy nor at high energy. It should be noted that although the differ-

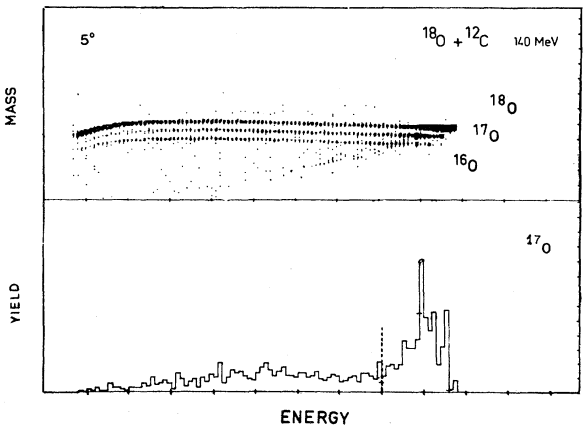

FIG. 5. The two dimensional mass versus energy spectrum reported in the upper part of the figure has been obtained for the $^{18}O + ^{12}C$ reaction at $E_{lab} = 140$ MeV and $\theta_{lab} = 5°$, by setting a window on the $Z = 8$ component of the ΔE versus energy spectrum. In the lower part of the figure the corresponding energy projection of the mass 17 component (^{17}O) and the cutoff between direct and compound contributions is indicated.

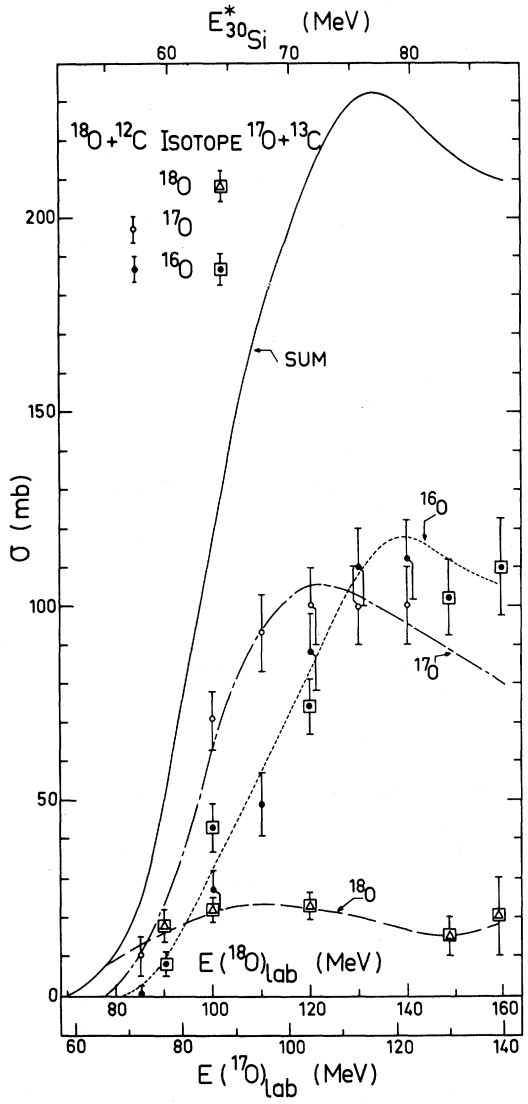

FIG. 6. The individual oxygen fusion evaporation isotope contributions ($3\alpha\chi n$ channels) extracted as indicated for both reactions are reported along with the sum of the three curves.

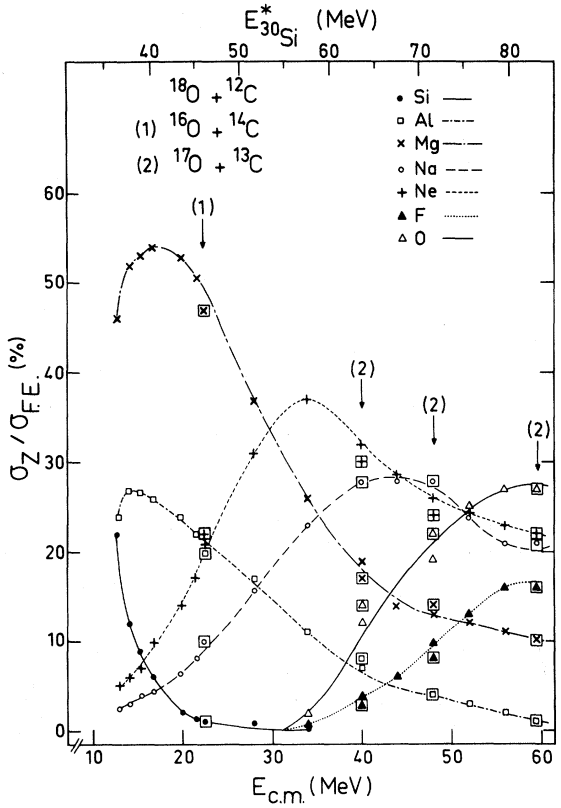

FIG. 7. Experimental relative cross sections versus center of mass bombarding energies for the $^{18}O + ^{12}C$ fusion evaporation element residues. Results for the $^{16}O + ^{14}C$ (1) and $^{17}O + ^{13}C$ (2) are reported at the corresponding excitation energies in the compound nucleus ^{30}Si. Relative errors of 5% on each relative cross section are not reported for simplicity reasons.

ence in Q values is small between $^{18}O + ^{12}C$ and $^{16}O + ^{14}C$ (+ 934 keV), it is much more important for the $^{17}O + ^{13}C$ channel (more than 3 MeV). The interest of the present work arises particularly in the fact that we have been able to compare the formation of each residual isotope, because the agreement in Fig. 7 could be fortuitous as the atomic numbers are the same in all entrance channels. In Fig. 9 the cross sections for all isotopes are compared for $E^*(^{30}Si) = 64$ MeV, where the results for $^{18}O + ^{12}C$ and $^{17}O + ^{13}C$ are seen to be identical within the experimental errors. The same excellent agreement is found at higher energies as well as for the $^{16}O + ^{14}C$ channel, which tends to prove that the reaction proceeds by a compound nucleus which is well equilibrated in all degrees of freedom.

All the cross sections for complete fusion are given in Figs. 10 and 11 as a function of $E_{c.m.}$ and are compared with the data of Eyal *et al.*[17] and Sperr *et al.*[10] for $^{18}O + ^{12}C$, and Wieleczko *et al.*[4] for $^{17}O + ^{13}C$. These curves will be commented on in detail during the discussion which compares a certain number of existing models.

The result obtained for the cross section of the direct channels are shown in Fig. 12, isotope by isotope in a Z-N space representation, for the $^{17}O + ^{13}C$ reaction at 130 MeV and $^{18}O + ^{12}C$ at 140 MeV. At these energies the grazing angular momenta are practically identical in the two reactions (Table I). The absolute values shown in Fig. 12 have been obtained by integrating over the measured angular range ($\theta \leq 20°$); these are, therefore,

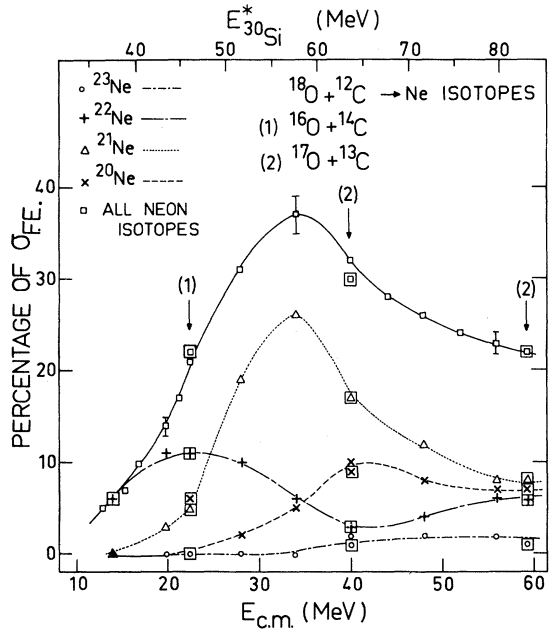

FIG. 8. Experimental relative cross sections versus center of mass bombarding energies for the $^{18}O + ^{12}C$ fusion evaporation neon isotopes. The corresponding results for the $^{16}O + ^{14}C$ (1) and $^{17}O + ^{13}C$ (2) are reported.

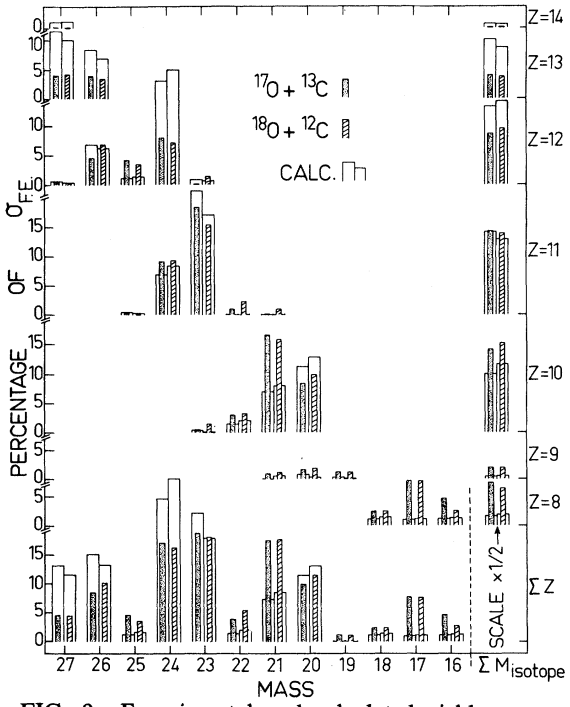

FIG. 9. Experimental and calculated yield comparison for the $^{18}O + ^{12}C$ ($E_{lab} = 100$ MeV) and $^{17}O + ^{13}C$ ($E_{lab} \simeq 85$ MeV) reactions corresponding to the same excitation energy of $E^* \simeq 64$ MeV in the compound nucleus ^{30}Si. A mass versus Z map representation is used along with the corresponding sums.

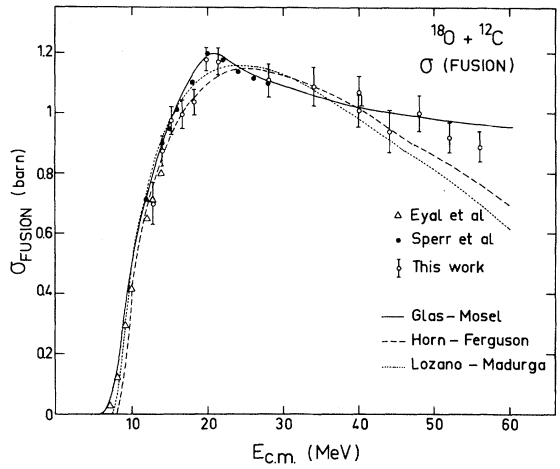

FIG. 10. Fusion cross section versus center of mass energy plot for the $^{18}O + ^{12}C$ reaction along with the predictions of three theoretical models discussed in the text.

not the absolute total cross section for the direct channels, although the angular ranges covered ($\theta_{c.m.} \lesssim 50°$) are so similar that comparison between the two reactions is justified. In the case where the direct exit channel corresponds to the projectile, we have proceeded as for the fusion cross sections and have supposed that the cross sections to the same exit channel are identical in both reactions. This last point will be justified in the discussion.

DISCUSSION

A. Hauser-Feshbach statistical model

The results for the fusion-evaporation products have been analyzed in the framework of the Hauser-Feshbach formalism using the Monte Carlo

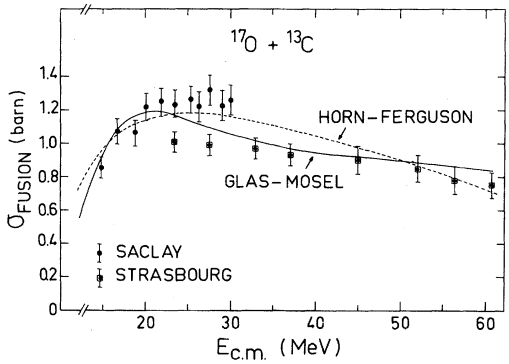

FIG. 11. Fusion cross section versus center of mass energy plot for the $^{17}O + ^{13}C$ reaction along with predictions of two models discussed in the text.

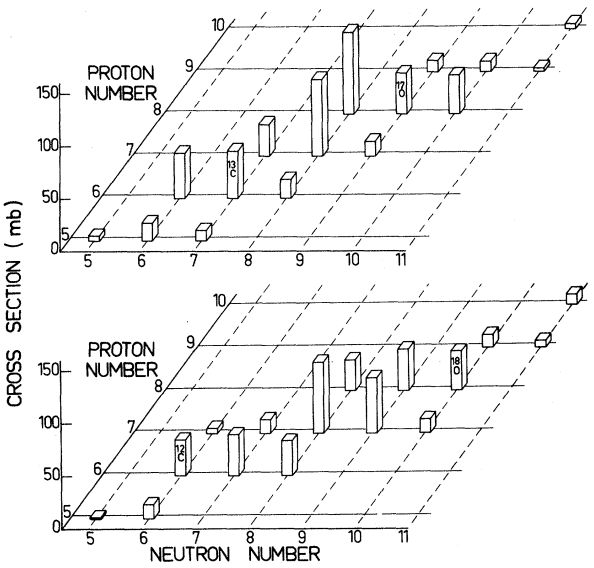

FIG. 12. Three dimensional neutron number—proton number—direct process cross-section representation for the ^{18}O (140 MeV) + ^{12}C and ^{17}O (130 MeV) + ^{13}C reactions corresponding nearly to the same grazing angular momentum: $l_g \simeq 31\hbar$.

code LILITA.[18] The calculations (histograms in Fig. 4) give a good qualitative description of the experimental spectra for products which are relaxed in energy, and help to decide where the cut should be applied with respect to the direct interactions. Towards the lower atomic numbers the average energy of the residual nuclei decreases and their width increases, consistent with the characteristic properties of a fusion-evaporation mechanism. It is important to show that the compound nucleus is formed independently of the entrance channel. The overall agreement found between experiment and theory, as illustrated in Figs. 9 and 13, is evidence in favor of a strongly equilibrated compound nucleus which decays in a statistical manner independent of the way in which it was formed. Certain differences appear for the ^{21}Ne and ^{24}Mg isotopes, where the theoretical predictions are inverted compared to experiment. Similar differences have been noted in other reactions, where the statistical model tends to overestimate the evaporation of nucleons at the expense of several alpha particles. For example, in the present case, the $3\alpha X n$ channels to oxygen isotopes are badly underestimated. We dismissed the

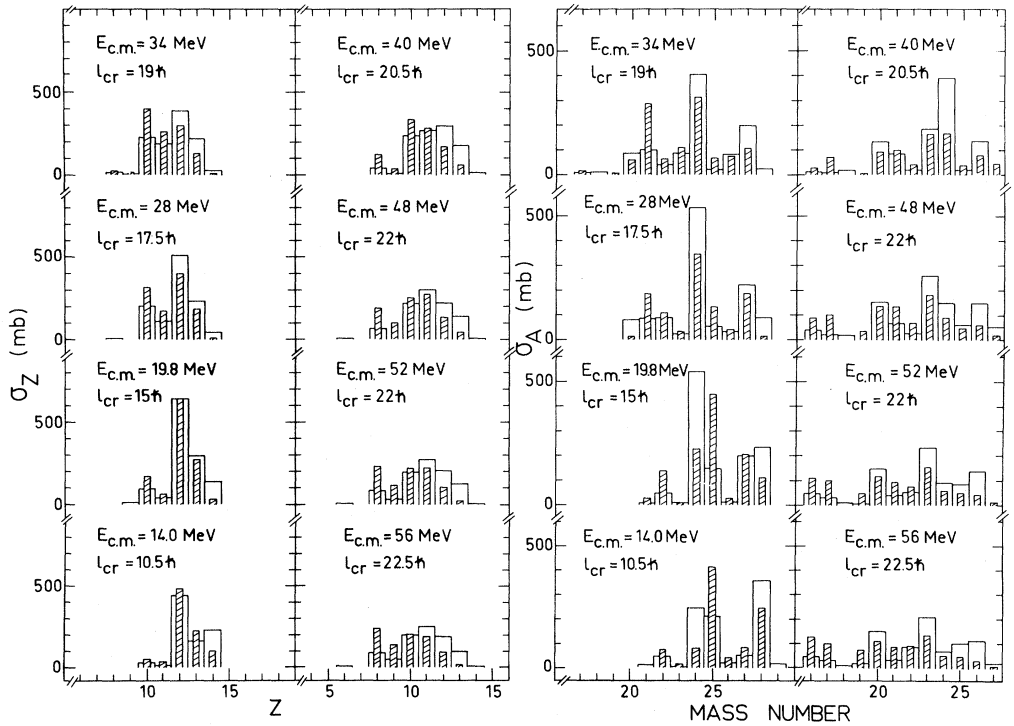

FIG. 13. Experimental (cross-hatched rectangles) and calculated (large white rectangles) cross sections for the $^{18}O + {}^{12}C$ reaction at eight bombarding energies covering the whole bombarding energy range. On the left hand side are plotted the Z spectra and on the right hand side the mass spectra.

possibility of an important preequilibrium contribution[16] in these reactions, but we have been forced to admit in our study of the C + C reactions[11] that no code can perfectly predict the distributions of evaporation residues at the higher energies.

B. Fusion cross section systematics

Two types of models have been proposed to account for the saturation of σ_{fus}, one based on entrance effects, the other on the properties of the compound nucleus. The models of critical distance,[5–7] where it is supposed that all partial waves which reach a critical distance R_c fuse, belong to the first category. When the two nuclei approach each other they feel the nucleus-nucleus interaction and the competition between the conservative and dissipative forces comes into play. The friction forces convert the kinematic into intrinsic energy of excitation. When the energy loss is sufficient this dinuclear structure becomes trapped in the potential well and interacts for a sufficiently long time that the system forgets its initial structure and fuses. The cross sections are well described by the general relationship

$$\sigma_{\text{fus}}(E_{\text{c.m.}})=\pi R^2\left[1-\frac{V(R)}{E_{\text{c.m.}}}\right] . \tag{1}$$

The radius R is given by

$$R=r(A_1^{1/3}+A_2^{1/3}) , \tag{2}$$

where r depends on the energy region. In the low energy region (~ 1 to 2 times the Coulomb barrier B_C) the reaction is dominated by the interaction barrier which depends essentially on the dynamics of the entrance channel, i.e., the specific properties of the target and projectile nuclei. Gutbrod *et al.*[19] found the value $r=1.4$ fm for this region. In the higher energy region, where the nuclei must penetrate into each other sufficiently before a compound nucleus can be formed, a value $r=1.0$ fm has been found by Galin *et al.*[5] We have fitted our results to the predictions of the phenomenological model of Glas and Mosel[7] which is applicable over the whole energy range.

$$\sigma_{\text{fus}}(E_{\text{c.m.}})=\frac{\hbar\omega R_B^{\,2}}{2E_{\text{c.m.}}}\ln\left[\frac{1+\exp[2\pi(E_{\text{c.m.}}-V_B)/\hbar\omega]}{1+\exp\left\{\frac{2\pi}{\hbar\omega}[E_{\text{c.m.}}-V_B-(E_{\text{c.m.}}-V_C)R_C^{\,2}/R_B^{\,2}]\right\}}\right] , \tag{3}$$

where $R_B(V_B)$ and $R_C(V_C)$ are the interaction and critical radii, respectively, and their associated potentials. For the $^{18}O + {}^{12}C$ reaction the Glas and Mosel fit in Fig. 10 was calculated with the parameters proposed by Schiffer.[10] The agreement is excellent over the whole energy range up to $E_{\text{lab}}=130$ MeV, where the contribution from the direct channels becomes stronger.[20] The experimental results for the $^{17}O + {}^{13}C$ reaction (Fig. 11) were fitted using a similar set of parameters using a critical radius $r_c=1.00$ fm. Although the agreement with our points at high energies is satisfactory, the Saclay data[4] between $20\leq E_{\text{c.m.}}\leq 30$ MeV are not reproduced very well. It should be pointed out that our results are in disagreement with the values reported by Wieleczko *et al.*[4] for which an $r_c=1.28$ fm value would be required to fit the data. A macroscopic model like this does not include shell effects, since such a description requires a more sophisticated treatment where one has to take into account the individual structure of each ion of the incident channel and the competition between fusion and other reaction channels. In the critical distance models it is difficult to understand intuitively the origin and physical nature of the parameters V_C and R_C. Horn and Ferguson[21] have avoided this problem and have simulated the nuclear structure by introducing into formula (1) a variable parameter ρ instead of the fixed distance R.

$$\sigma_{\text{fus}}(E_{\text{c.m.}})=\pi\rho(\rho-D) , \tag{4}$$

where $D=Z_1Z_2e^2/E$ is the collision distance

$$\rho=mE+b . \tag{5}$$

The contact distance b contains information on the structure of the target projectile nuclei as it is taken equal to the sum of the radii at 1.35% of the charge density at the center of the nuclei (cf. De Jager *et al.*[22]). The coefficient $m=d\rho/dE$ depends only on the mass of the compound nucleus and is given by the empirical form

$$m^{-1}=18[2.23-(A_1+A_2)^{1/3}] . \tag{6}$$

Acceptable fits are found in Figs. 10 and 11 considering the uncertainties inherent in the choice of

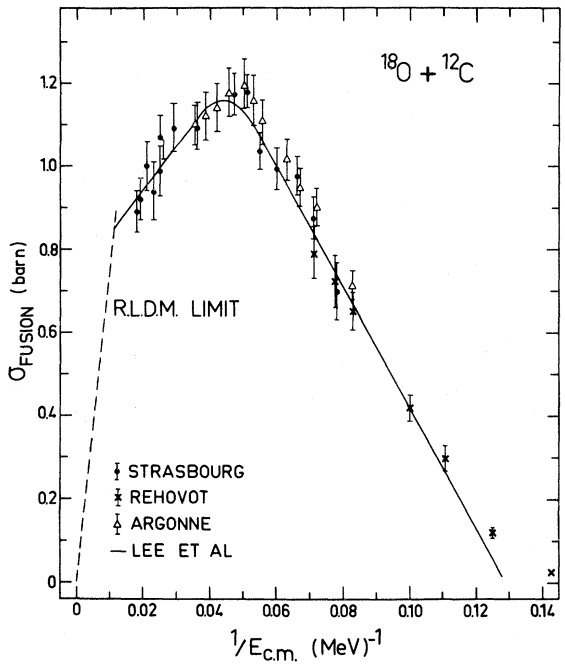

FIG. 14. Fusion cross section versus $1/E_{c.m.}$ for the $^{18}O + ^{12}C$ reaction. The solid line correspond to the prediction of the statistical yrast line model of Lee *et al.* (Ref. 3). The RLDM limit is indicated.

parameters. The prescription of Lozano and Madurga[23] is similar to that of Horn and Ferguson but differs in the choice of the contact distance b, which is defined as the sum of the radii, where the nuclear density is equal to 0.002 nucleons f_m^{-3}. Naturally, both models give similar results, as shown for the $^{18}O + ^{12}C$ reaction in Fig. 10. At the higher energies they drop below the experimental values and the predictions of Glas and Mosel. However, the main weakness of these empirical models is that they do not successfully reproduce the break in cross sections as a function of $1/E_{c.m.}$ that is so evident in Fig. 14. This is also true for the friction models based on a proximity model[24] and for the time dependent Hartree-Fock (TDHF) (Ref. 25) calculations which give a good qualitative agreement up to a certain energy ($E_{max} \simeq 2B_C$), but beyond which the sudden drop in cross section is not predicted in a satisfactory manner.

In the second generation of fusion models the limitation due to the yrast line of the compound nucleus has been introduced as in the work of Glas and Mosel[26] and then Harar.[27] Here the fusion cross section is limited by the number of high spin states available in the compound nucleus. Lee *et al.*[8] interpreted the fusion cross sections at high energy in terms of a statistical yrast line which lies parallel to the conventional yrast line at an additional energy ΔQ:

$$E_{y,st} = \frac{\hbar^2}{2I} l_{CR}(l_{CR}+1) + \Delta Q \ , \tag{7}$$

where the compound nucleus A is assumed to be a rigid sphere of radius $R = R_0 A^{1/3}$ with moment of inertia $I = I_{rig} = \frac{2}{5} A R^2$. Using the sharp cutoff approximation one arrives finally at an expression applicable in the second region:

$$\sigma_{fus}(E_{c.m.}) = (\pi I/\mu)[1 + (Q - \Delta Q)/E_{c.m.}] \ , \tag{8}$$

where $\mu = A_1 A_2/(A_1 + A_2)$ and Q the binding energy of the system. For the first region σ_{fus} is taken as equal to σ_R. In the $^{18}O + ^{12}C$ reaction the values $\Delta Q = 10$ MeV and $r_0 = 1.2$ fm have been adopted. Figure 4 shows the remarkable agreement which is obtained up to the highest energy. For the

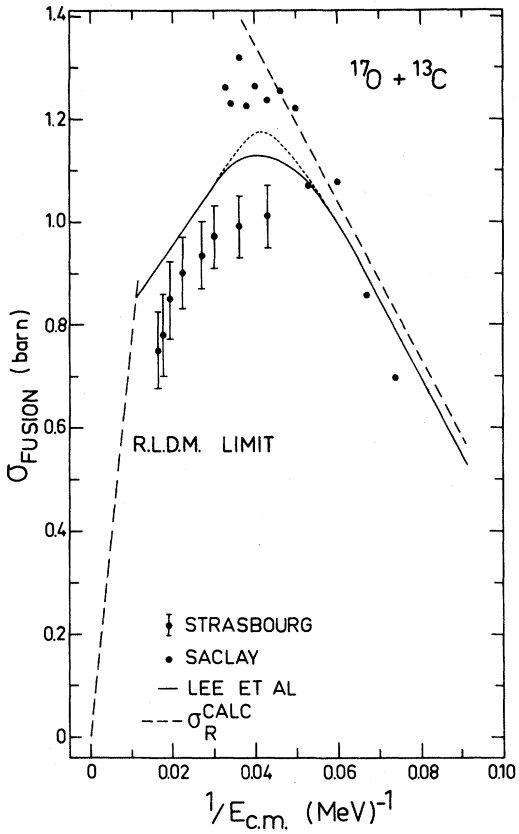

FIG. 15. Fusion cross section versus $1/E_{c.m}$ for the $^{17}O + ^{13}C$. The solid line corresponds to the prediction of the statistical yrast line model of Lee *et al.* (Ref. 3) and the channel spin effect in these calculations appear in the central part of the curve as the small dotted to the full line difference. The RDLM limit is indicated. The total reaction cross section calculated with the code GENOA is reported.

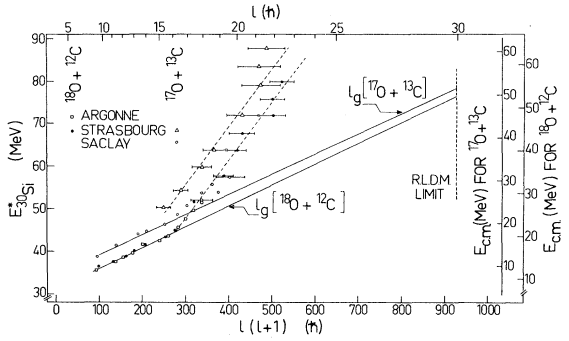

FIG. 16. Critical angular momentum $[l(l+1)]$ versus excitation energy representation for the $^{18}O + ^{12}C$ and $^{17}O + ^{13}C$ reactions. The grazing angular momenta for both systems are plotted. The dotted lines are guides to the eye, with a slope corresponding to the moment of inertia of ^{30}Si considered as a rigid sphere.

$^{17}O + ^{13}C$ reaction the results shown in Fig. 15 are compared with calculations using the same parameters. The effect of the channel spin (Fig. 15: dotted line to full line) in this case is to slightly depress the experimental values of σ_{fus}.[28] We have already remarked that the Saclay results are in serious disagreement with our total fusion cross sections. If the Saclay values were correct it would imply that the fusion cross section is practically equal to the total reaction cross section (Fig. 15), and consequently the direct reaction cross section should be very small. This is in conflict with what we have observed both in particle and γ ray studies.[29] For example, for the intensity of the $^{18}O\ 2^+ \rightarrow 0^2\ \gamma$ transition alone, cross sections greater than 50 mb were observed[29] for $15 \leq E_{c.m.} \leq 25$ MeV, where the contribution of fusion processes is negligible. Although we are not sure about the reasons for the discrepancy, this would suggest that the Saclay cross sections are overestimated.

To discern how the properties of the compound nucleus ^{30}Si could effect the reaction mechanism we have represented E^*_{CN} against l_{CR} in the conventional $l(l+1)$ representation, for the fusion results of $^{18}O + ^{12}C$ and $^{17}O + ^{13}C$ in Fig. 16. The resulting curves can be interpreted in the following way:

(a) In the first region ($E^* < 45$ MeV) the interaction barrier is the dominant effect and $l_{CR} = l_{graz}$ ($\Delta Q = 3.098$): Fusion is governed by entrance channel conditions.

(b) In the intermediate region ($45 \leq E^* \leq 80$ MeV) the two channels behave similarly. The slope of the dotted lines, drawn through the experimental points to guide the eye, corresponds to the moment of inertia of ^{30}Si considered as a rigid sphere. They are shifted with respect to each other because of the 10% difference in cross section. However, the points correspond to conditions in the compound nucleus where the level density is sufficient ($10^3 \leq \rho \leq 10^4$ levels/MeV) for fusion to take place. In this respect we note that the criterion for the formation of a compound nucleus in the model proposed by Vandenbosch and Lazzarini[30] is that the distance between levels for a given angular momentum J should be comparable or less than their width: $\Gamma_J / D_J \leq 1$. A very similar and even stronger difference in fusion cross sections of $^{10}B + ^{16}O$ and $^{12}C + ^{14}N$, leading to the neighboring compound nucleus ^{26}Al, has been observed by Gomez del Campo *et al.*[2,31] in this same so-called second regime of fusion. Very recently, Chan *et al.*[32] reported a similar effect for the reactions $^{10}B + ^{17}O$ and $^{12}C + ^{15}N$ leading to the same compound nucleus ^{27}Al.

(c) At higher energies ($E^* > 70$ MeV) the behavior of the two systems appears to converge, although the limit to the stability of ^{30}Si has not been reached in contrast to the ^{26}Al case.[2,31] The limit ($l = 30\hbar$), reported on Fig. 16, corresponds to the vanishing of the fission barrier calculated with the RLDM.[9] One should, however, point out that this fission barrier drops under the particle thresholds ($\simeq 10$ MeV for neutrons or α) for $l \simeq 22\hbar$; therefore, even if "conventional fission" would not take place for such a light compound nucleus as ^{30}Si, a new degree of freedom for the deexcitation is open; one is probably already concerned with the deep inelastic region where the difference between the quasielastic and longer processes becomes less distinct.

C. Direct channels analysis

Although the physical origin of the saturation of σ_{fus} has not yet been clarified, the important point is that at high energy there exists a critical angular momentum l_{CR} appreciably less than the grazing angular momentum l_g. The question arises as to what happens to the flux in these partial waves between l_{CR} and l_g.

The isotope distributions for the direct reaction products (Fig. 12) for the $^{18}O + ^{12}C$ and $^{17}O + ^{13}C$ reactions show similarities even though the mass asymmetry is different in the entrance channels. This is emphasized by the representation of Fig. 17 where the direct cross sections are reported versus the number of particles transferred to the projectile, at low as well as high bombarding energy. It should

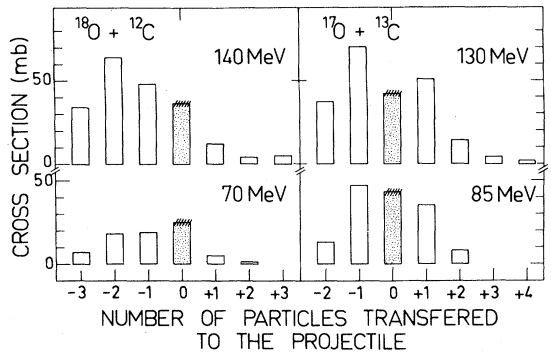

FIG. 17. Direct reaction cross sections versus the number of particles transferred to the projectile for ^{18}O (70 and 140 MeV) + ^{12}C and ^{17}O (85 and 130 MeV) + ^{13}C. The hatched bars indicate that the projectile direct reaction cross-section contributions are taken from the other reaction (see text).

be noted that, for the same grazing angular momentum, the $^{17}O + ^{13}C$ direct reaction cross section is $\simeq 10\%$ higher than for $^{18}O + ^{12}C$ ($\theta_{c.m} \leq 51°$) than for $^{17}O + ^{13}C$ ($\theta_{c.m.} \leq 46°$). This difference between both reactions is also supported by our low energy γ-ray measurements[33] ($E_{lab} \leq 80$ MeV). The isotope distributions (Figs. 12 and 17) are probably due to the superposition of fast processes corresponding to different degrees of damping in these most peripheral collisions. On one hand, partial mass equilibration takes place explaining, for example, formation of ^{15}N in the case of $^{18}O + ^{12}C$ (a strong three-nucleon transfer is unlikely). On the other hand, one observes that many more elements further removed from the target and projectile are formed in the $^{17}O + ^{13}C$ reaction. It would mean, as has also been suggested by Gomez del Campo *et al.*,[31] that the incident flux which does not fuse ($l_{cr} \leq l \leq l_g$) is evacuated by these direct channels. Very recently, Tabor *et al.*[34] suggested that fragmentation phenomena of the projectile could occur and they report a total amount of 330 mb for 141 MeV ^{18}O on ^{12}C. Such contributions in our direct channel data can surely not be ruled out; however, only precise exclusive particle-heavy ion coincidence measurements could distinguish between the different possible reaction mechanisms.

The fact that the direct channels are more intense in the $^{17}O + ^{13}C$ reaction compared to $^{18}O + ^{12}C$ can explain the differences observed for fusion (Fig. 16), since the flux missing from the fusion-evaporation processes of $^{17}O + ^{13}C$ would be absorbed into the direct channels where there are open channels available. This explanation follows along the same line of reasoning developed by Haas and Abe[35] on the origin of the resonant structures observed experimentally, for the reactions $^{18}O + ^{12}C$ (Ref. 33) and $^{16}O + ^{14}C$,[36] for example. The number of open channel calculations predicts not only the existence of a molecular resonance region[20] but also how the flux of the reaction would be portioned in the various exit channels.[16]

CONCLUSION

The study of the $^{17}O + ^{13}C$ and $^{18}O + ^{12}C$ reactions has shown that at incident energies corresponding to the second region of fusion there is an appreciable difference in the cross sections for complete fusion and those for deep inelastic processes (of several degrees of relaxation) confirming an entrance channel effect. It is suggested that the effect of channel spin is not sufficient to explain this difference but rather that it is owing to the difference in the availablity of open channels as suggested by Haas and Abe.

This work has shown that at high incident energies it is important to identify each isotope formed in order to determine all contributions to the cross sections and to extract, in particular, the values of the critical angular momenta for fusion. The estimation of the compound nucleus and direct contributions, at high energies, has been facilitated by the Hauser-Feshbach statistical model which predicts the form of the energy spread of the evaporation residues which, in consequence, aids the choice of the cut in energy which separates them from the direct products. Experiment and comparison with the calculation of the evaporation code LILITA have demonstrated the existence of a compound nucleus ^{30}Si, which is strongly equilibrated in all its degrees of freedom and decays in a statistical manner independent of the entrance channel by which it was formed. These calculations cannot be expected to perfectly reproduce the partition into all exit channels, as the nuclear structure and deformation effects have not been incorporated into the theory in a satisfactory fashion.

It appears from recent results that after a certain energy threshold, precompound emission or fragmentation of the projectile cannot be neglected. We have not considered them in this work because they would not explain the difference in the complete fusion cross sections between $^{18}O + ^{12}C$ and $^{17}O + ^{13}C$. In spite of these uncertainties it would appear that the formation of the compound nucleus ^{30}Si is limited from an angular momentum for which the fission barrier is smaller than the minimum binding energy of the nucleons in the nucleus. It would be informative to study the same compound nucleus ^{30}Si through a symmetric chan-

nel $^{15}N + ^{15}N$ and by an asymmetric channel $^{19}F + ^{11}B$.

ACKNOWLEDGMENTS

We would like to thank Prof. S. M. Lee of the University of Tsukuba with whom we have had long and fruitful discussions. In particular, we would like to thank him for the calculations concerning the statistical yrast line model which were done in collaboration with Dr. Matsuse, and for careful reading of the manuscript.

[1]D. G. Kovar, D. F. Geesaman, T. H. Braid, Y. Eisen, W. Henning, T. R. Ophel, M. Paul, K. E. Rehm, S. J. Sanders, P. Sperr, J. P. Schiffer, S. L. Tabor, S. Vigdor, B. Zeidman, and F. W. Prosser, Jr., Phys. Rev. C 20, 1305 (1979), and references therein.

[2]J. Gomez del Campo, R. G. Stokstad, J. A. Biggerstaff, R. A. Dayras, A. H. Snell, and P. H. Stelson, Phys. Rev. C 19, 2170 (1979).

[3]S. M. Lee, Y. Higashi, Y. Nagashima, S. Hanashima, M. Sato, H. Yamaguchi, M. Yamanouchi, and T. Matsuse, Phys. Lett. 98B, 421 (1981).

[4]J. P. Wieleczko, S. Harar, M. Conjeaud, and F. Saint-Laurent, Phys. Lett. 93B, 35 (1980).

[5]J. Galin, D. Guerreau, M. Lefort, and X. Tarrago, Phys. Rev. C 9, 1018 (1974).

[6]R. Bass, Nucl. Phys. A231, 45 (1974).

[7]D. Glas and U. Mosel, Nucl. Phys. A237, 429 (1975); Phys. Rev. C 10, 2620 (1974).

[8]S. M. Lee, T. Matsuse, and A. Arima, Phys. Rev. Lett. 45, 165 (1980).

[9]S. Cohen, F. Plasil, and W. J. Swiatecki, Ann. Phys. (N.Y.) 82, 557 (1974).

[10]P. Sperr, T. H. Braid, Y. Eisen, D. G. Kovar, F. W. Prosser, Jr., J. P. Schiffer, S. L. Tabor, and S. Vigdor, Phys. Rev. Lett. 37, 321 (1976); J. P. Schiffer, in Proceedings of Colloque Franco-Japonais de Spectrosopie Nucléaire et Réaction Nucléaire Dogashima, 1976 (unpublished), p. 176.

[11]B. Heusch, C. Beck, J. P. Coffin, R. M. Freeman, A. Gallmann, F. Haas, F. Rami, P. Wagner, and D. E. Alburger, Phys. Rev. C 23, 1527 (1981).

[12]A. Gobbi, R. Wieland, L. Chua, D. Shapira, and D. A. Bromley, Phys. Rev. C 7, 30 (1973).

[13]F. G. Perey (unpublished), modified version by B. S. Nilsson.

[14]M. P. Webb, Ph.D. thesis, University of Washington, Seattle, 1976 (unpublished).

[15]J. P. Coffin, P. Engelstein, A. Gallmann, B. Heusch, P. Wagner, and H. E. Wegner, Phys. Rev. C 17, 1607 (1978).

[16]B. Heusch, C. Beck, J. P. Coffin, R. M. Freeman, A. Gallmann, F. Haas, F. Rami, P. Wagner, and D. E. Alburger, J. Phys. C 10, 229 (1980).

[17]Y. Eyal, M. Beckerman, R. Chechik, Z. Fraenkel, and H. Stocker, Phys. Rev. C 13, 1527 (1976).

[18]Description and use of the Monte Carlo code LILITA, J. Gomez del Campo and R. G. Stokstad, Oak Ridge National Laboratory, Report ORNL/TM-7295, 1981.

[19]H. H. Gutbrod, W. G. Winn, and M. Blann, Nucl. Phys. A213, 267 (1973).

[20]Y. Abe, in *Proceedings of the International Conference on Resonant Behavior of Heavy Ion Systems, Aegean Sea (Greece) 1980,* edited by G. Vourvopoulos *et al.* (National Printing Office, Athens, 1981); Research Institute for Fundamental Physics, Kyoto University Reports RIFP 421 and 428, 1981 (unpublished).

[21]D. Horn and A. J. Ferguson, Phys. Rev. Lett. 41, 1529 (1978).

[22]C. W. De Jager, H. De Vries, and C. De Vries, At. Data Nucl. Data Tables 14, 479 (1974).

[23]M. Lozano and G. Madurga, Phys. Lett. 90B, 50 (1980); M. Lozano, G. Madurga, and P. H. Hodgson, *ibid.* 82B, 170 (1979).

[24]J. Randrup, Ann. Phys. (N.Y.) 112, 356 (1978); J. R. Birkelund, L. E. Tubbs, J. R. Huizenga, J. N. De, and D. Sperber, Phys. Rep. 56, (1979) 107; L. C. Vaz and J. M. Alexander, Phys. Rev. C 18, 2152 (1978); K. Nagatani and J. C. Peng, *ibid.* 19, 747 (1979); R. Vandenbosch, Nucl. Phys. A339, 167 (1980).

[25]S. J. Krieger and K. T. R. Davies, Phys. Rev. C 20, 167 (1979).

[26]D. Glas and U. Mosel, Phys. Lett. 78B, 9 (1978).

[27]S. Harar, in *Nuclear Molecular Phenomena,* edited by N. Cindro (North-Holland, Amsterdam, 1978), p. 329.

[28]T. Matsuse, A. Arima, T. Tsukamoto, and S. M. Lee, contributed Abstract to the International Conference on Nuclear Physics, Berkeley, 1980, LBL Report No. LBL-11118, 1980; S. M. Lee and T. Matsuse, private communication.

[29]R. M. Freeman, in *Proceedings of the International Conference on the Resonant Behavior of Heavy Ion Systems, Aegean Sea (Greece), 1980,* edited by G. Vourvopoulos *et al.* (National Printing Office, Athens, 1981).

[30]R. Vandenbosch and A. J. Lazzarini, Phys. Rev. C 23, 1074 (1981).

[31]J. Gomez del Campo, R. A. Dayras, J. A. Biggerstaff, D. Shapira, A. H. Snell, P. H. Stelson, and R. G. Stokstad, Phys. Rev. Lett. 43, 26 (1979).

[32]Y. D. Chan, D. E. Digregorio, J. L. C. Ford, Jr., J. Gomez del Campo, M. E. Ortiz, and D. Shapira, Bull. Am. Phys. Soc. 26, 554 (1981).

[33]R. M. Freeman, C. Beck, F. Haas, B. Heusch, and J. J. Kolata (unpublished); R. M. Freeman and F. Haas, Phys. Rev. Lett. 40, 927 (1978); Z. Basrak, C. Beck, R. Caplar, R. M. Freeman, and F. Haas, Fizika 13, 33 (1981).

[34]S. L. Tabor, L. C. Denis, K. W. Kemper, J. D. Fox, K. Abdo, G. Neuschaefer, D. G. Kovar, and H. Ernst, Phys. Rev. C 24, 960 (1981).

[35]F. Haas and Y. Abe, Phys. Rev. Lett. 46, 1667 (1981).

[36]J. J. Kolata, C. Beck, R. M. Freeman, F. Haas, and B. Heusch, Phys. Rev. C 23, 1056 (1981).